Dalton Transactions

Accepted Manuscript

ROYAL SOCIETY OF CHEMISTRY

www.rsc.org/dalton

A new visible light excitable ICT-CHEF mediated fluorescence 'turn on' probe for the selective detection of Cd^{2+} in mixed aqueous system with live-cell imaging

Shyamaprosad Goswami, *[a] Krishnendu Aich, [a] Sangita Das, [a] Chitrangada Das Mukhopadhyay, [a] Deblina Sarkar [b] and Tapan Kumar Mondal [b]

Graphical Abstract:

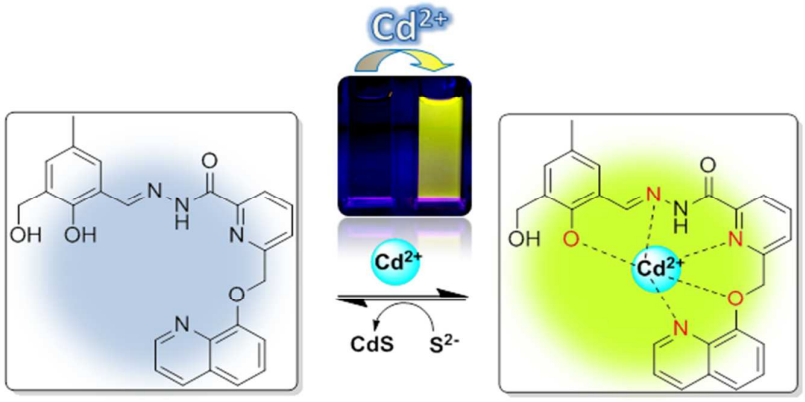

Journal Name

RSCPublishing

ARTICLE

A new visible light excitable ICT-CHEF mediated fluorescence 'turn on' probe for the selective detection of Cd^{2+} in mixed aqueous system with live-cell imaging

Cite this: DOI: 10.1039/xoxxoooooox

Received ooth January 2012,
Accepted ooth January 2012

DOI: 10.1039/xoxxoooooox

www.rsc.org/

Shyamaprosad Goswami, *[a] Krishnendu Aich, [a] Sangita Das, [a] Chitrangada Das Mukhopadhyay, [b] Deblina Sarkar [c] and Tapan Kumar Mondal [c]

A new quinoline based sensor was developed and applied for selective detection of Cd^{2+} both *'in vitro'* and *'in vivo'*. The designed probe displays a straightforward approach for the selective detection of Cd^{2+} with a prominent enhancement of fluorescence along with a large red shift (~ 38 nm), which may because of the CHEF (chelation enhanced fluorescence) and ICT (internal charge transfer) process after interaction with Cd^{2+}. The interference from other biologically important competing metal ions especially Zn^{2+} has not been observed. The visible light excitability of the probe merits in the view point of its biological application. The probe enables to detect intracellular Cd^{2+} with non-cytotoxic effect which was demonstrated with the live RAW cells. The experimentally observed change in structure and electronic properties of the sensor after addition of Cd^{2+} were modelled by Density Functional Theory (DFT) and Time Dependent Density Functional Theory (TDDFT) computational calculations, respectively. Moreover, the test strip experiment with this sensor exhibits both absorption and fluorescence color changes when exposed to Cd^{2+} in mixed aqueous solution which also makes the probe more useful. The minimum limit of detection of Cd^{2+} by the probe was in the range of 9.9×10^{-8} M level.

Introduction

Detection and imaging of biologically relevant target molecules through fluorescence in living systems has emerged as an area of intense interest in the chemistry-biology interface owing to its significant biomedical implications.[1] Specially the development of fluorescent chemosensors for sensing and reporting heavy transition-metal (HTM) ions has been receiving considerable attention in recent years.[2] Fluorescent probes are designed and synthesised in such a way that after interaction with the analytes they exhibit a drastic change in the emission profile, which ultimately show turn-on or shifts in the emission maxima. This phenomenon is guided by few proposed mechanisms like intermolecular charge transfer (ICT),[3] chelation-induced enhanced fluorescence (CHEF),[4] photo-induced electron transfer (PET),[5] excimer/exciplex formation,[6] excited-state intramolecular proton transfer,[7] and fluorescence resonance energy transfer (FRET)[8] etc. Out of them CHEF induced fluorescence change is very important as metal ions have tendency to form chelate with the organic donor ligands.[9] When the CHEF process is in switch-on condition, the conjugation increases drastically which leads to enhancement in the emission. On the other hand, due to the binding with the metal ions the ICT mechanism is facilitated over the π-system. This also caused sufficient enhancement in the fluorescence. CHEF and ICT mediated probes for the detection of heavy metal ions are limited and so there exists a significant room for improvement. HTM ions, in particular Cd^{2+}, have received immense attention due to their harmful effects on public health. As Cd^{2+} has been widely used in agriculture, industry [10] and the military for centuries, it can be easily introduced in our body through air, food, water or through inhaling the cigarette smoke. Recent studies indicate that human exposure to cadmium may cause lung, renal and prostate cancers and calcium metabolism disorders.[11] However, the mechanism involved in the Cd^{2+} carcinogenesis remains undefined.[12] The EPA (United States Environmental Protection Agency) gives an affordable drinking water standard for Cd^{2+} of 5 ppb to prevent the diseases caused by Cd^{2+} exposure. The WHO (World Health Organization) also provides a maximum limit of 3 ppb of Cd^{2+} for drinking water.[13] Consequently, the development of a method for the quantification of Cd^{2+} in environmental samples as well as in living beings is of great significance to suppress the Cd^{2+}-carcinogenesis. Thus, extensive research efforts have been

devoted in recent years and many fluorescent sensors for Cd^{2+} have been documented in literature.[14] However, some limitations hamper their practical applications. Most of them have low water solubility, poor detection limit and the excitation and emission wavelengths are in the UV region, which limits their practical biological applications. For '*in vivo*' imaging, the excitability of the sensor lies in the visible or NIR (near infra red) region which are most appropriate to suppress the autofluorescence, photo bleaching and photo damage of the biological samples. Therefore, there is a critical demand to develop the sensors especially which are easily synthesizable and have long excitation wavelength to promote the *'in vivo'* imaging is an interested area of the sensing research.

In continuation of our work, in the field of sensor developement, [15] herein, we report a new visible light excitable sensor to monitor Cd^{2+} selectively both *'in vitro'* and *'in vivo'* with non-cytotoxic properties. The recognition of Cd^{2+} was investigated by absorption, emission, ^{1}H NMR and HRMS spectroscopy techniques. Further DFT and TDDFT calculations were performed to investigate the mechanism. Moreover detection of cadmium *'in vivo'* in live RAW 264.7 cells under confocal microscopy has also been demonstrated in this study.

Experimental

General

Unless otherwise mentioned, materials were obtained from commercial suppliers and were used without further purification. Thin layer chromatography (TLC) was carried out using Merck 60 F_{254} plates with a thickness of 0.25 mm. Melting points were determined on a hot-plate melting point apparatus in an open-mouth capillary and are uncorrected. ^{1}H and ^{13}C NMR spectra were recorded on JEOL 400 MHz and 100 MHz instruments respectively. For NMR spectra, $CDCl_3$ and d_6-DMSO were used as solvents using TMS as internal standard. Chemical shifts are expressed in δ units and ^{1}H–^{1}H and ^{1}H–C coupling constants in Hz. UV-vis spectra were recorded on a JASCO V-630 spectrometer. Fluorescence spectra were recorded on a Perkin Elmer LS 55 fluorescence spectrometer. IR spectra were recorded on a JASCO FT/IR-460 plus spectrometer, using KBr discs. For the titration experiment, we use the cations viz. [Na^+, K^+, Ca^{2+}, Ni^{2+}, Mn^{2+}, Zn^{2+}, Cd^{2+}, Cu^{2+}, Fe^{3+}, Cr^{3+}, Pb^{2+}, Hg^{2+}] as their chloride salts and Al^{3+} as its nitrate salt.

General method of UV-vis and fluorescence titration

UV-vis method

For UV-vis titrations, stock solution of the receptor (10 μM) was prepared in [(CH_3CN / water), 2/3, *v/v*] (at 25°C) using PBS buffered solution. The solutions of the guest cations using their chloride salts in the order of 1×10^{-5} M, were prepared in deionized water using PBS buffer at pH = 7.3. Solutions of various concentrations containing the sensor and increasing concentrations of cations were prepared separately. The spectra of these solutions were recorded by means of UV-vis method.

Fluorescence method

For fluorescence titrations, stock solution of the sensor (10 μM) used was the same as that used for UV-vis titration. The solutions of the guest cations using their chloride salts in the order of 1×10^{-5} M, were prepared in deionised water. Solutions of various concentrations containing sensor and increasing concentrations of cations were prepared separately. The spectra of these solutions were recorded by means of fluorescence method.

Determination of fluorescence quantum yield

To determine the quantum yields of BPQ and BPQ-Cd^{2+}, we recorded their absorbance in methanol solution. The emission spectra were recorded using the maximal excitation wavelengths, and the integrated areas of the fluorescence-corrected spectra were measured. The quantum yields were then calculated by comparison with fluorescein (Φ_s = 0.97 in basic ethanol) as reference using the following equation:

$\Phi_x = \Phi_s \times (I_x/I_s) \times (A_s/A_x) \times (n_x/n_s)^2$

where, x & s indicate the unknown and standard solutions respectively, Φ is the quantum yield, I is the integrated area under the fluorescence spectra, A is the absorbance and n is the refractive index of the solvent.

Synthetic method for the preparation of the probe

To the suspension of compound A (0.2 g, 0.682 mmol) in ethanol, 2-hydroxy-3-(hydroxymethyl)-5-methylbenzaldehyde (0.1 g, 0.682 mmol) was added with continuous stirring. The reaction mixture was then refluxed for 6 hours. After ensuring that the reactants were fully consumed, the reaction mixture was allowed to cool to room temperature. A white precipitate appeared which was filtered, washed with cold ethanol (1ml × 2) and dried in air. Yield = (0.24 g) 82%.

Mp =142-145^{0}C.

^{1}H NMR (400 MHz, $CDCl_3$): δ 2.20 (s, 3H), 5.44 (s, 4H), 7.0 (d, *J*= 8 Hz, 4H), 7.41 (m, 4H), 7.72 (d, *J*= 8Hz, 2H), 6.332 (s, 2H), 6.628 (s, 2H), 6.896 (dd, *J*=7.05 Hz,1H), 7.80 (t, *J*=8 Hz, 2H), 8.13 (dd, 2H), 8.53 (dd, 2H), 8.95 (t, *J*=8 Hz,1H), 11.29 (s, 1H), 11.64 (s, 1H).

^{13}C NMR (100 MHz, $CDCl_3$): δ 20.2, 30.9, 70.9, 110.0, 119.6, 120.7, 121.9, 122.1, 124.9, 126.7, 128.8, 129.7, 131.6, 136.2, 138.5, 140.3, 147.6, 148.7, 149.6, 153.9, 155.6, 156.0, 159.9.

HRMS (ESI, positive): calcd. for $C_{25}H_{23}N_4O_4$ $[M + H]^+$ (m/z): 443.1719; found: 443.1536.

Synthesis of Cd^{2+} complex (BPQ-Cd^{2+}) of receptor

The receptor, BPQ (50 mg) and $CdCl_2$ (14 mg) were mixed together and dissolved in 5 ml of methanol. After reflux for 12 hours the reaction mixture was cooled to room temperature. A reddish-yellow coloured precipitate appeared which was filtered and dried in vacuum.

HRMS (ESI, Positive): calcd. for $C_{25}H_{22}CdClN_4O_4$ $[M + Cd^{2+} + Cl^-]^+$ (m/z): 591.0352; found: 591.1286.

Computational method

Full geometry optimizations were carried out using the density functional theory (DFT) method at the B3LYP[16-18] level for the compounds. All elements except cadmium were assigned 6-31+G(d) basis set. The LANL2DZ basis set with effective core potential (ECP) set of Hay and Wadt[19] was used for Cd^{2+}-complex. The vibrational frequency calculations were performed to ensure that the optimized geometries represent the local minima and there were only positive eigen values. Vertical electronic excitations based on B3LYP optimized geometries were computed using the time-dependent density functional theory (TDDFT) formalism[20-22] in methanol using conductor-like polarizable continuum model (CPCM).[23-25] All calculations were performed with Gaussian 09 program package [26] with the aid of the Gauss View visualization program.

Details of live-cell imaging

Materials Methods

Frozen Human colorectal carcinoma cell line **HCT 116 (ATCC : CCL-247)** were obtained from the American Type Culture Collection (Rockville, MD, USA) and maintained in Dulbecco's modified Eagle's medium (DMEM, Sigma Chemical Co., St. Louis, MO, USA) supplemented with 10% fetal bovine serum (Invitrogen), penicillin (100 µg/ml), and streptomycin (100 µg/ml). The RAW 264.7 macrophages were obtained from NCCS, Pune, India and maintained in DMEM containing 10% (v/v) fetal calf serum and antibiotics in a CO_2 incubator. Cells were initially propagated in 25 cm^2 tissue culture flask in an atmosphere of 5% CO_2 and 95% air at 37°C humidified air till 70- 80% confluency.

Fluorescent imaging studies

For fluorescent imaging studies, RAW cells**,** 7.5×10^3 cells in 150 µl media were seeded on sterile 12 mm diameter Poly L lysine coated cover-slip and kept in a sterile 35mm covered Petri dish and incubated at 37°C in a CO_2 incubator for 24-30 h. Next day cells were washed three times with phosphate buffered saline (pH 7.4) and fixed using 4% paraformaldehyde in PBS (pH 7.4) for 10 minutes at room temperature washed with PBS followed by permeabilization using 0.1% saponin for 10 minutes. Then the cells were incubated with 20 µM $CdCl_2$ dissolved in 100 µl DMEM at 37 °C for 1 h in a CO_2 incubator and observed under epifluorescence microscope (Carl Zeiss). The cells were again washed thrice with PBS (pH 7.4) to remove any free metal and incubated in DMEM containing probe (BPQ) to a final concentration of 1.1×10^{-6} M followed by washing with PBS (pH 7.4) three times to remove excess probe outside the cells. Again, images were taken using epifluorescence microscope. Before fluorescent imaging aspirate out all the solutions and mounted on slides in a mounting medium containing DAPI (1µg/ml) and stored in dark before microscopic images are acquired.

Cytotoxicity assay

The cytotoxic effects of the probe, $CdCl_2$ and probe−$CdCl_2$ complex were determined by an MTT assay following the manufacturer's instruction (MTT 2003, Sigma-Aldrich, MO). HCT cells were cultured into 96-well plates (approximately 10^4 cells per well) for 24 h. Next day media was removed and various concentrations of probe, $CdCl_2$ and probe−$CdCl_2$ complex (0, 15, 25, 50, 75, and 100 µM) made in DMEM were added to the cells and incubated for 24 h. Solvent control samples (cells treated with DMSO in DMEM), no cells and cells in DMEM without any treatment were also included in the study. Following incubation, the growth media was removed, and fresh DMEM containing MTT solution was added. The plate was incubated for 3−4 h at 37°C. Subsequently, the supernatant was removed, the insoluble colored formazan product was solubilized in DMSO, and its absorbance was measured in a microtiter plate reader (Perkin-Elmer) at 570 nm. The assay was performed in triplicate for each concentration of probe, $CdCl_2$ and probe−$CdCl_2$ complex. The OD value of wells containing only DMEM medium was subtracted from all readings to get rid of the background influence. Data analysis and calculation of standard deviation was performed with Microsoft Excel 2007 (Microsoft Corporation).

Results and discussion

Design and synthesis

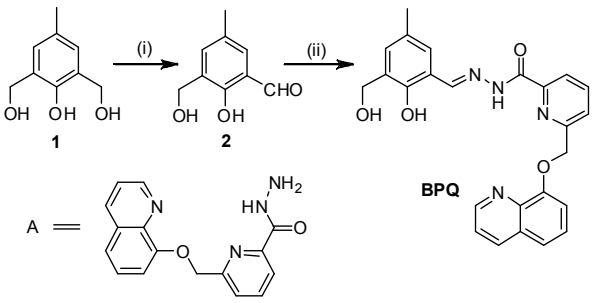

Scheme 1. Reagents and conditions: (i) MnO_2, $CHCl_3$, reflux, 12 h, 56%; (ii) A, EtOH, reflux, 6 h, 82%.

The synthetic scheme of the probe (BPQ) is shown below (Scheme 1). Compound A is prepared by adopting literature procedure, previously reported by us.[14h] As depicted in Scheme 1, compound **2** [2-hydroxy-3-(hydroxymethyl)-5-methylbenzaldehyde] was synthesized by mono-oxidation of compound **1** using MnO_2 in $CHCl_3$. By treatment of compound **2** with compound A in ethanol afforded the probe as white solid in 82% yield. The structure of BPQ was confirmed by ^1H NMR, ^{13}C NMR and HRMS spectroscopy (ESI, Fig. S12-S16).

Absorption and emission studies of BPQ

Absorption studies

The photophysical properties of BPQ were carried out in an optimized CH_3CN- PBS buffer (2/3, *v/v*, pH = 7.3) solution. In

UV-vis titration of BPQ with Cd^{2+} exhibited a colour change from colorless to light yellow. No other (Na^{+}, K^{+}, Ca^{2+}, Ni^{2+}, Mn^{2+}, Zn^{2+}, Cd^{2+}, Cu^{2+}, Fe^{3+}, Cr^{3+}, Pb^{2+}, Al^{3+}, Hg^{2+}) analyte does succeed any notable distortion in UV-vis profile (Fig. 1b). Even higher Zn^{2+} concentration does not lead to any further change. In the absorbance profile, BPQ (10 μM) itself shows two maxima at 307 nm and 365 nm. Upon incremental addition of Cd^{2+} (0-30μM) the peak at 307 nm gradually decreases and consequently two new bands appear at 355 nm and 460 nm (Fig. 1a).

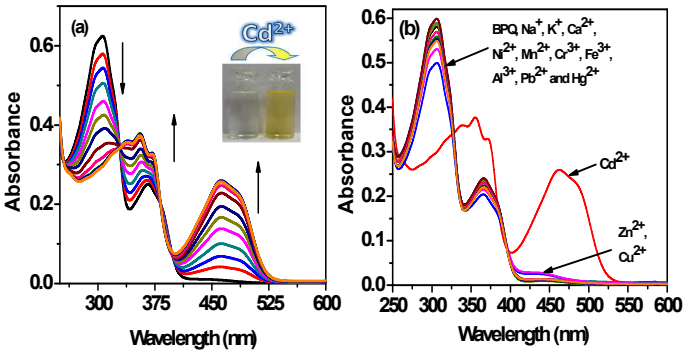

Figure 1: (a) Change of absorption spectra of BPQ (10 μM) upon gradual addition of Cd^{2+} (0 to 30 μM). Inset: Photograph showing the visible color change of BPQ before and after addition of Cd^{2+} (20 μM). (b) Changes of absorption spectra of BPQ (10 μM) upon addition of stated metal ions (30 μM).

As a result two clear isosbestic points come into view at 330 and 383 nm. The change in color of chemosensor BPQ upon addition of Cd^{2+} was clearly visible under visible light by the naked-eye (Fig. 1a, Inset) whereas in the presence of the other metal ions the metal–ligand solution was remain colorless. This is an interesting feature by which we can detect Cd^{2+} without using any other instrumental technique. Upon interaction with Cd^{2+}, a prominent new absorbance band at 460 nm developed and upon incremental addition of Cd^{2+} the peak at 460 nm rapidly increased. During the addition of Cd^{2+} the absorption ratio (A_{460}/A_{307}) exhibits a good linear curve of fitness with added Cd^{2+} concentration (1.1 to 11.7 μM, Fig S4a, ESI) with a R^2 value of 0.9933. The association constant for the Cd^{2+} complexation with BPQ was estimated to be 7.82×10^4 M^{-1} from Benesi-Hildebrand plot using the data obtained from UV-vis titration (Fig. S2, ESI).

To verify the selectivity of BPQ towards Cd^{2+}, competition experiment was performed. To execute this experiment, absorbance data were recorded at 460 nm after addition of different guest analytes (30 μM) to the solution of BPQ (CH_3CN/H_2O, 2/3, v/v, pH =7.3, PBS Buffer) in presence of Cd^{2+} (Fig. S6).

Fluorescence studies

The emission spectra of BPQ and its fluorescence titration with Cd^{2+} were also recorded in CH_3CN- PBS buffer (2/3, *v/v*, pH = 7.3) solution. The fluorescence spectrum of BPQ (10 μM) exhibits a low emission at 512 nm upon excitation at 430 nm. Upon addition of a small amount of aqueous Cd^{2+} solution to the solution of BPQ, the fluorescence emission at 512 nm is red-shifted (~ 38 nm) to 550 nm, (Fig. 2a) this change may be due to the internal charge transfer (ICT). The incremental addition of Cd^{2+} (0 – 20 μM) to the solution of BPQ, leads to a dramatic enhancement of the fluorescence intensity at 550 nm, which is attributed to the chelation-induced enhance fluorescence (CHEF). The fluorescence quantum yield of the sensor was increased from 0.02 to 0.46 in the presence of 2 equivalents of Cd^{2+} (ESI). Accordingly, the fluorescence of BPQ clearly changed from 'turn-off' to yellow after addition of Cd^{2+}, which was observed through naked eye after illumination under UV light (Fig. 2a, Inset).

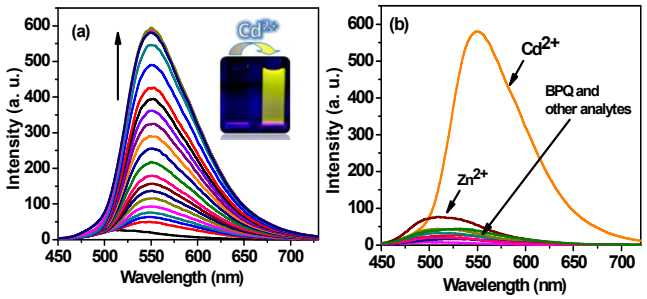

Figure 2: (a) Change of emission spectra of BPQ (10 μM) upon gradual addition of Cd^{2+} (0 to 20 μM). Inset: visible emission observed from BPQ in absence and presence of 20 μM of Cd^{2+}, taken under UV light. (b) Change of fluorescence spectra of BPQ after addition of different metal ions stated. λ_{ex} = 430 nm.

Here Cd^{2+} forms a stable chelate with BPQ as shown in scheme 2. Notably, addition of other co-existing metal ions, even in an excess amount to the sensor, caused insignificant changes in the emission intensity of the receptor (Fig. 2b). For Zn^{2+}, a slight increase of fluorescence intensity was observed. But the twist is the interference which occurs at different wavelength (506 nm). This is possibly due to the similar chemical properties of Cd^{2+} and Zn^{2+}. A good linear relationship was observed between fluorescence intensity (550 nm) and added concentration of Cd^{2+} from 0 – 9.5 μM (Fig. S4b, ESI). The association constant was determined to be 1.55×10^5 M^{-1}, using the data obtained from fluorescence titration. To determine the limit of detection i.e how lower concentration of Cd^{2+} can be determined by the probe (BPQ), we recorded the fluorescence data starting from the Cd^{2+} concentration as low as 10^{-8} M using 1 μM solution (CH_3CN/H_2O, 2/3, v/v, pH =7.3, PBS Buffer) of BPQ (Fig S1, ESI). Now from the concentration dependent fluorescence titration experiment we can see that minimum 9.9×10^{-8} M Cd^{2+} can enhance the fluorescence intensity of BPQ at 550 nm. Thus, the detection limit of BPQ was found to be 9.9×10^{-8} M for Cd^{2+}.

Mechanism of Cd^{2+} sensing

The enhancement in the fluorescence intensity of BPQ after addition of Cd^{2+} is possibly attributed to two very important mechanisms one is ICT and the other is CHEF. Firstly, BPQ

itself exhibits a low fluorescence intensity which may be due to the free rotation of the imine (-C=N) bond. But after introduction of Cd^{2+}, this free rotation inhibits because the metal ion induced chelation takes place by involving the binding site of the probe BPQ (–OH group, imine N-atoms and the two heterocyclic donor segments). The introduction of Cd^{2+} makes the system more rigid; consequently, both the mechanisms play the key role for this fluorescence enhancement.

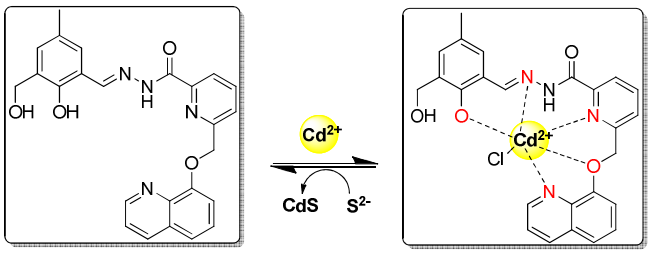

Scheme 2. Proposed binding mode of BPQ with Cd^{2+}

This also caused sufficient enhancement in the fluorescence for the binding mechanism from the ICT point of view. The CHEF phenomenon in conjunction with the ICT process upon interacting with Cd^{2+}, perhaps results in the enhancement in the fluorescence intensity of the free receptor along with a red shift of ~ 38 nm. The proposed CHEF mechanism was verified through the HRMS spectra of BPQ-Cd^{2+} complex. The stoichiometry of this complexation (BPQ-Cd^{2+}) fits satisfactorily with the relationship of 1:1 (host-guest) binding model, which is supported by the Job's plot diagram (Fig. S5, ESI). The HRMS spectrum of BPQ exhibits a peak at *m/z* 443.1536 possibly for $[BPQ + H]^+$ whereas for the BPQ-Cd^{2+} complex shows a peak at *m/z* 591.1286 may be due to $[BPQ + Cd^{2+} + Cl^-]^+$, which also proves the mononuclear complex of BPQ with Cd^{2+} (Fig. S19, ESI). We have recorded ^1H NMR spectra of the probe (BPQ) with various concentrations of Cd^{2+} in d^6 DMSO containing 1% D_2O. From the NMR data, it was observed that the peak arises at δ 12.36 ppm which gradually disappears upon addition of Cd^{2+}. This observation indicates the binding of the probe with Cd^{2+} (Fig. S17).

Sensing of Cd^{2+} using TLC plate

Efforts were made to examine the binding of Cd^{2+} with the receptor BPQ in the solid state. In order to investigate a practical application of this sensor, an experiment called "dip-stick" method was performed. It is a very simple but very important experiment because it gives instant qualitative information without resorting to the instrumental analysis. In order to perform this experiment we have prepared BPQ solution for inspecting Cd^{2+} in CH_3CN solution of BPQ (2×10^{-4} M) and then drying it in the air. Now to investigate Cd^{2+}, we immersed the TLC plate to Cd^{2+} (2×10^{-4} M) solution and then exposing it in air to evaporate the solvent.

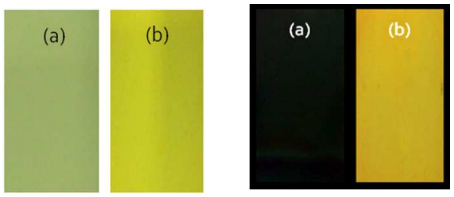

Figure 3: Photographs of TLC plates after immersion in a BPQ-acetonitrile solution (a) and after immersion in a BPQ-Cd^{2+}–acetonitrile solution (b) taken in ambient light (left) and under hand-held UV light (right).

Now the colour of the TLC plates change from light green to yellowish green and under UV light turn-off to yellow (Fig. 3). This experiment evokes a real time monitoring and is devoid of using any instrumental analysis, just via naked-eye detection and using of TLC plates we can easily investigate a qualitative instant detection of Cd^{2+}.

Reversibility of RHP

It is a well known fact that reversibility is an important criterion for an excellent chemical sensor. Thus, the chemical reversibility behavior of BPQ was studied to examine the reusability of the receptor. The reversibility is very important parameter to evaluate the performance of a receptor. To check whether the complexation process is reversible or not, emission titration experiments were performed using the BPQ-Cd^{2+} complex with S^{2-}. From the titration experiment, it is clear that the fluorescence was quenched and the original BPQ spectra are restored. The light yellow colour of the BPQ-Cd^{2+} solution was dispersed while colorless solution was noticed with simultaneous addition of S^{2-} (Fig S7, ESI). It indicates the decomplexation of BPQ-Cd^{2+} as S^{2-} strips away Cd^{2+} from the binding zone.

pH study

Now from the acid–base titration experiment with the probe in hand exposed that BPQ does not undergo any notable change in the fluorescence profile within the pH range from 2–9, this investigation suggests that the molecule is stable in this pH range. But in strong basic conditions (pH > 9), deprotonation of the phenolic group causes the coloration along with strong yellow fluorescence (Fig. S8, ESI). Thus BPQ can be employed for the detection of Cd^{2+} in near-neutral pH range (pH = 7.3).

Computational study

To further understand the relationship between the structural changes of BPQ and its complex with Cd^{2+} and the optical response of BPQ to Cd^{2+}, we carried out density functional theory (DFT) and time dependent density functional theory (TDDFT) calculations with the B3LYP/6-31+G(d) method basis set using the Gaussian 09 program. The optimized geometry and the highest occupied molecular orbital (HOMO) and lowest unoccupied molecular orbital (LUMO) of BPQ and its Cd^{2+} complex are presented in Fig. 4.

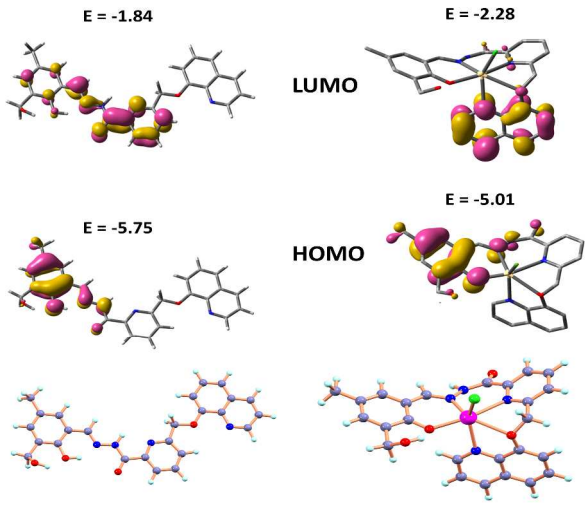

Figure 4: Energy diagrams of HOMO and LUMO orbital's of BPQ and BPQ-Cd^{2+} complex calculated at the DFT level using a B3LYP/6-31+G(d) basis set.

UV-vis spectra of BPQ and its Cd complex were calculated using the TDDFT method in methanol medium. Calculated absorption peaks had agreed well with the experimentally observed peaks (ESI, Table S1). In case of BPQ, the transition from HOMO to LUMO and HOMO – 2 to LUMO had contributed mainly to the excitation at 357 nm and 308 nm respectively (ESI, Table S1). For the Cd^{2+} complex, main absorption peaks were at 442 nm and 363 nm generated from the transition of HOMO to LUMO and HOMO to LUMO + 2.

Cell viability assay

Considerations the thermodynamic favourable binding properties of BPQ with Cd^{2+} practical application that lead to the further examination of the ability of the probe (BPQ) to sense Cd^{2+} in the living cells. In order to fulfil this objective it is important to determine the cytotoxic effect of BPQ and Cd^{2+} and the complex on live cells. The well-established MTT assay, which is based on mitochondrial dehydrogenase activity of viable cells, was adopted to study cytotoxicity of above mentioned compounds at varying concentrations mentioned in method section. Figure 5 shows that probe compound did not exert any adverse effect on cell viability; same is the case when cells were treated with varying concentrations of $CdCl_2$.
However, exposure of HCT cells to Probe–Cd complex resulted in a decline in cell viability above 20 µM concentration.
The effect was more pronounced in higher concentration and showed an adverse cytotoxic effect in a dose-dependent manner. The viability of HCT cells was not influenced by the solvent (DMSO) as evidenced in Figure 5, leading to the conclusion that the observed cytotoxic effect could be attributed to Probe- Cd^{2+} complex. The results obtained in the in vitro cytotoxic assay suggested that, in order to pursue fluorescence imaging studies of Probe- cadmium complex in live cells, it would be prudent to choose a working concentration of 20 µM for probe compound. Hence, to assess the effectiveness of compound BPQ as a probe for intracellular detection of Cd^{2+} by fluorescence microscopy, RAW cells were treated with 20 µM $CdCl_2$ for 1 h followed by 10 µM probe solution to promote formation of probe - cadmium complex. On the basis of the established 1:1 stoichiometry of binding between BPQ and Cd^{2+}, it can be reasonably assumed that the concentration of the complex formed in HCT cells would be much lower than the concentration (20 µM) at which a marginal cytotoxic effect of the complex was observed (Figure 5).

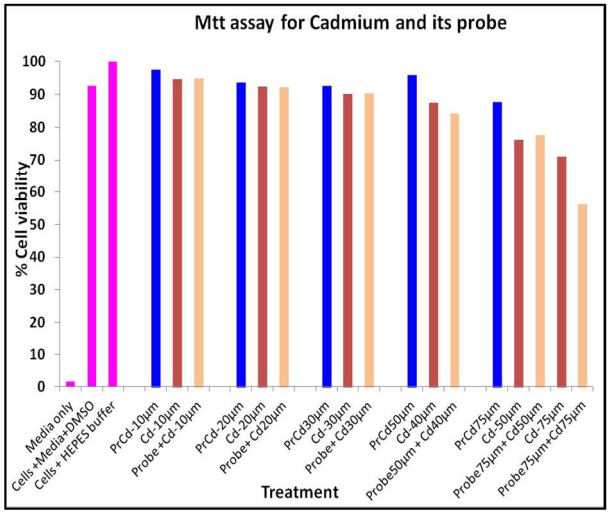

Figure 5: It represents % cell viability of HCT cells treated with different concentrations (10 µM-70 µM) of BPQ for 12 hrs determined by MTT assay. Results are expressed as mean of three independent experiments.

Fluorescent imaging of live-cells

Fluorescence microscopic studies revealed a lack of fluorescence for RAW cells when treated with either probe compound or $CdCl_2$ alone (Figure 6, panel a and b). Upon incubation with $CdCl_2$ followed by probe compound a striking switch-on fluorescence was observed inside RAW cells, which indicated the formation of Probe- cadmium complex, as observed earlier in solution studies. Further, an intense green fluorescence was conspicuous in the perinuclear region of RAW cells (Figure 6, panel b) which indicates that the probe can penetrate cell membrane easily and can be used to probe Cd in cells. The fluorescence microscopic analysis strongly suggested that probe compound could readily cross the membrane barrier, permeate into RAW cells, and rapidly sense intracellular Cd^{2+}. It is significant to mention here that bright field images of treated cells did not reveal any gross morphological changes, which suggested that RAW cells were viable. These findings open up the avenue for future *in vivo* biomedical applications of the sensor.

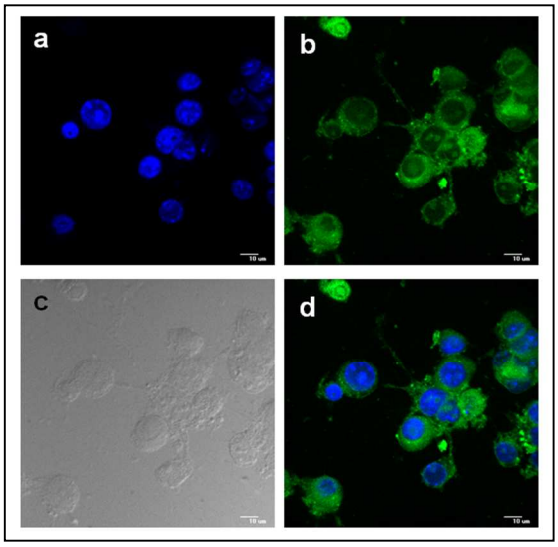

Figure 6: Confocal microscopic images of probe in RAW 264.7 cells pretreated with $CdCl_2$: (a) $CdCl_2$ treatment only at 20 μM concentration, nuclei counterstained with DAPI (1 μg/ml), (b) treatment a followed by probe BPQ at concentration 1.1×10^{-6} M, (c) bright field image of the cells after treatment (d) overlay image in dark field. All images were acquired with a 40× objective lens.

Conclusions

In summary, a fluorescent sensing system based on pyridine - hydroxyquinoline moieties has been successfully designed and synthesized. This visible light excitable probe employed ICT and CHEF strategies into one system to obtain a highly efficient fluorescent molecular switch for specific detection of Cd^{2+}. Addition of incremental analyte concentration exhibits a remarkable emission enhancement accompanying with a red-shift in the emission maxima along with a visible colour change from colorless to light yellow. This probe could afford a high selectivity and sensitivity to Cd^{2+} over metal ions of interest particularly Zn^{2+} with a very low detection limit of 0.56 ppb in physiological conditions. This complextation was further examined by DFT and TDDFT calculations. Also to demonstrate its value in practical applications, bio-imaging was successfully performed by HCT cells. The probe was applied to detect the intracellular Cd^{2+} in live-cells.

Acknowledgements

Authors thank the CSIR and DST, Govt. of India for financial supports. K.A, S.D and D.S acknowledge CSIR for providing them fellowships.

Notes and references

[a] Department of Chemistry, Indian Institute of Engineering Science and Technology, Shibpur, Howrah-711 103, India. Fax: +91 33 2668 2916; Tel: +91 33 2668 2961-3; E-mail: spgoswamical@yahoo.com
[b] Department of Centre for Healthcare Science & Technology, Indian Institute of Engineering Science and Technology, Shibpur, Howrah-711 103, India
[c] Department of Chemistry, Jadavpur University, Kolkata, India .

† Footnotes should appear here. These might include comments relevant to but not central to the matter under discussion, limited experimental and spectral data, and crystallographic data.

Electronic Supplementary Information (ESI) available: [details of any supplementary information available should be included here]. See DOI: 10.1039/b000000x/

1. (a) P. N. Prasad, *Introduction to Biophotonics,* Wiley, NJ, 2003; (b) J. B. Pawley, *Handbook of Biological Confocal Microscopy,* Plenum, New York, 1995; (c) J. W. Lichtman and J.-A. Conchello, *Nat. Methods*, 2005, **2**, 910.
2. (a) J. P. Desvergne, A. W. Czarnik, *Chemosensors of Ion and Molecule Recognition*; Kluwer: Dordrecht, 1997; (b) B. Valeur, I. Leray, *Coord. Chem. Rev*. 2000, **205**, 3; (c) A. P. de Silva, H. Q. N. Gunaratne, T. Gunnlaugsson, A. J. M. Huxley, C. P. McCoy, J. T. Rademacher, T. E. Rice, *Chem. Rev*. 1997, **97**, 1515; (d) Y. Zhou, Z.-X. Li, S.-Q. Zang, Y.-Y. Zhu, H.-Y. Zhang, H.-W. Hou and T. C. W. Mak, *Org. Lett*., 2012, **14**, 1214; (e) Y. Fu, Q.-C. Feng, X.-J. Jiang, H. Xu, M. Li and S.-Q. Zang, *Dalton Trans*. 2014, **43**, 5815; (f) X.-J. Jiang, Y. Fu, H. Tang, S.-Q. Zang, H.-W. Hou, T. C.W. Mak, H.-Y. Zhang, *Sens. Actuators B*, 2014, **190**, 844.
3. (a) Z. Xu, Y. Xiao, X. Qian, J. Cui and D. Cui, *Org. Lett*., 2005, **7**, 889; (b) J. B. Wang, X. F. Qian and J. N. Cui, *J. Org. Chem*., 2006, **71**, 4308; (c) S. Goswami, S. Das and K. Aich, *Tetrahedron Lett*., 2013, **54**, 4620; (d) S. Goswami, K. Aich, S. Das, A. K. Das, D. Sarkar, S. Panja, T. K. Mondal and S. K. Mukhopadhyay, *Chem. Commun*., 2013, **49**, 10739
4. (a) N. C. Lim, J. V. Schuster, M. C. Porto, M. A. Tanudra, L. Yao, H. C. Freake and C. Bruckner, *Inorg. Chem*., 2005, **44**, 2018; (b) S. Goswami, S. Das, K. Aich, D. Sarkar, T. K. Mondal, C. K. Quah and H.-K. Fun, *Dalton Trans*., 2013, **42**, 15113
5. (a) T. Gunnlaugsson, A. P. Davis, J. E. O'Brien and M. Glynn, *Org. Lett*., 2002, **4**, 2449; (b) D. H. Vance and A. W. Czarnik, *J. Am. Chem. Soc*., 1994, **116**, 9397; (c) S. K. Kim and J. Yoon, *Chem. Commun*., 2002, 770.
6. (a) S. Nishizawa, Y. Kato and N. Teramae, *J. Am. Chem. Soc*., 1999, **121**, 9463; (b) J.-S. Wu, J.-H. Zhou, P.-F. Wang, X.-H. Zhang and S.- K. Wu, *Org. Lett*., 2005, **7**, 2133; (c) B. Schazmann, N. Alhashimy and D. Diamond, *J. Am. Chem. Soc.*, 2006, **128**, 8607; (d) A. Banerjee, A. Sahana, S. Guha, S. Lohar, I. Hauli, S. K. Mukhopadhyay, J. S. Matalobos and D. Das, *Inorg. Chem*., 2012, **51**, 5699.
7. S. Goswami, S. Das, K. Aich, B. Pakhira, S. Panja, S. K. Mukherjee and S. Sarkar, *Org. Lett.,* 2013, **15**, 5412.
8. (a) J. M. Serin, D. W. Brousmiche and J. M. J. Frechet, *J. Am. Chem. Soc.*, 2002, **124**, 11848; (b) A. E. Albers, V. S. Okreglak and C. J. Chang, *J. Am. Chem. Soc*., 2006, **128**, 9640; (c) S. H. Lee, S. K. Kim, J. H. Bok, S. H. Lee, J. Yoon, K. Lee and J. S. Kim, *Tetrahedron Lett*., 2005, **46**, 8163; (d) W. R. Dichtel, J. M. Serin, C. Edder, J. M. J. Frechet, M. Matuszewski, L.-S. Tan, T. Y. Ohulchanskyy and P. N. Prasad, *J. Am. Chem. Soc*., 2004, **126**, 538; (e) M. Suresh, S. Mishra, S. K. Mishra, E. Suresh, A. K. Mandal, A. Shrivastav and A. Das, *Org. Lett*., 2009, **11**, 2740; (f) P. Mahato, S. Saha, E. Suresh, R. D. Liddo, P. P. Parnigotto, M. T. Conconi, M. K. Kesharwani, B. Ganguly and A. Das,

Inorg. Chem., 2012, **51**, 1769; (g) K. Sreenath, J. Allen, R. M. W. Davidson and L. Zhu, *Chem. Commun*., 2011, **47**, 11730; (h) R. J. Wandell, A. H. Younes and L. Zhu, *New J. Chem*., 2010, **34**, 2176.

9. (a) A. M. Jane, M. S. Matin, T. Amy, M. H. John and A. N. Polly, *J. Natl. Cancer Inst*., 2006, **98**, 869; (b) A. Akesson, B. Julin and A. Wolk, *Cancer Res*., 2008, **68**, 6435.
10. R. L. Chaney, J. A. Ryan, Y.-M. Li and S. L. Brown, in *Cadmium in Soils and Plants*; ed. by M. J. McLaughlin, B. R. Singh, Kluwer: Boston, 1999, 219.
11. (a) G. Jiang, L. Xu, S. Song, C. Zhu, Q. Wu, L. Zhang and L. Wu, *Toxicology*, 2008, **244**, 49; (b) T. Jin, J. Lu, M. Nordberg, *Neurotoxicology.,* 1998, **19**, 529.
12. (a) S. Satarug, J. R. Baker, S. Urbenjapol, M. Haswell-Elkins, P. E. B. Reilly, D. J. Williams and M. R. Moore, *Toxicol. Lett.*, 2003, **137**, 65; (b) M. Waisberg, P. Joseph, B. Hale and D. Beyersmann, *Toxicology*., 2003, **192**, 95; (c) R. K. Zalups and S. Ahmad, *Toxicol. Appl. Pharmacol*., 2003, **186,** 163.
13. (a) United States Environmental Protectioin Agency, http://water.epa.gov/drink; (b) World Health Organization, Avenue Appia 20, 1211 Geneva 27, Switzerland, http://www.who.int/water_sanitation_health/dwq/chemicals/cadmium /en/.
14. (a) Y. Tan, J. Gao, J. Yu, Z. Wang, Y. Cui, Y. Yang and G. Qian, *Dalton Trans*, 2013, **42**, 11465; (b) L. Xu, M-L He, H-B Yang and X. Qian, *Dalton Trans*., 2013, **42**, 8218; (c) L.-K. Zhang, Q.-X. Tong and L.-J. Shi, *Dalton Trans*., 2013, **42**, 8567; (d) K. P. Divya, S. Savithri and A. Ajayaghosh, *Chem. Commun*., 2014, **50**, 6020; (e) Y. Xu, L. Xiao, S. Sun, Z. Pei, Y. Pei and Y. Pang, *Chem. Commun*., 2014, **50**, 7514; (f) L. Xue, C. Liu and H. Jiang, *Org. Lett*., 2009, **11**, 1655; (g) L. Xue, Q. Liu and H. Jiang, *Org. Lett*., 2009, **11**, 3454; (h) S. Goswami, K. Aich, S. Das, A. K. Das, A. Manna, S. Halder, *Analyst*, 2013, **138**, 1903; (i) S. Goswami, K. Aich, D. Sen. *Chem. Lett*. 2012, **41**, 863.
15. (a) S. Goswami, K. Aich, A. K. Das, A. Manna and S. Das, *RSC Adv*., 2013, **3**, 2412; (b) S. Goswami, S. Das, K. Aich, D. Sarkar and T. K. Mondal, *Tetrahedron Lett*. 2013, **54**, 6892; (c) S.Goswami, S. Das, K. Aich, D. Sarkar and T. K. Mondal, *Tetrahedron Lett.*, 2014, **55**, 2695; (d) S. Goswami, K. Aich, S. Das, S. B. Roy, B. Pakhira and S. Sarkar*, RSC Advances,* 2014, **4**, 14210.
16. A.D. Becke*, J. Chem. Phys*. 1993, **98**, 5648.
17. C. Lee, W. Yang and R. G. Parr, *Phys. Rev. B* 1988, **37**, 785.
18. D. Andrae, U. Haeussermann, M. Dolg, H. Stoll and H. Preuss, *Theor. Chim. Acta* 1990, **77**, 123.
19. P. J. Hay and W. R. Wadt, *J. Chem. Phys*. 1985, **82**, 299.
20. R. Bauernschmitt and R. Ahlrichs, *Chem. Phys. Lett.* 1996, **256**, 454.
21. R.E. Stratmann, G.E. Scuseria and M.J. Frisch, *J. Chem. Phys*. 1998, **109**, 8218.
22. M.E. Casida, C. Jamorski, K.C. Casida and D.R. Salahub, *J. Chem. Phys*. 1998, **108**, 4439.
23. V. Barone and M. Cossi, *J. Phys. Chem. A* 1998, **102**, 1995.
24. M. Cossi and V. Barone, *J. Chem. Phys*. 2001, **115,** 4708.
25. M. Cossi, N. Rega, G. Scalmani and V. Barone*, J. Comput. Chem*. 2003, **24**, 669.
26. Gaussian 09, Revision D.01, M. J. Frisch, G. W. Trucks, H. B. Schlegel, G. E. Scuseria, M. A. Robb, J. R. Cheeseman, G. Scalmani, V. Barone, B. Mennucci, G. A. Petersson, H. Nakatsuji, M. Caricato, X. Li, H. P. Hratchian, A. F. Izmaylov, J. Bloino, G. Zheng, J. L. Sonnenberg, M. Hada, M. Ehara, K. Toyota, R. Fukuda, J. Hasegawa, M. Ishida, T. Nakajima, Y. Honda, O. Kitao, H. Nakai, T. Vreven, J. A. Montgomery, Jr., J. E. Peralta, F. Ogliaro, M. Bearpark, J. J. Heyd, E. Brothers, K. N. Kudin, V. N. Staroverov, R. Kobayashi, J. Normand, K. Raghavachari, A. Rendell, J. C. Burant, S. S. Iyengar, J. Tomasi, M. Cossi, N. Rega, J. M. Millam, M. Klene, J. E. Knox, J. B. Cross, V. Bakken, C. Adamo, J. Jaramillo, R. Gomperts, R. E. Stratmann, O. Yazyev, A. J. Austin, R. Cammi, C. Pomelli, J. W. Ochterski, R. L. Martin, K. Morokuma, V. G. Zakrzewski, G. A. Voth, P. Salvador, J. J. Dannenberg, S. Dapprich, A. D. Daniels, Ö. Farkas, J. B. Foresman, J. V. Ortiz, J. Cioslowski and D. J. Fox, Gaussian, Inc., Wallingford CT, 2009.

